

## Effect of Turbulence Model in Numerical Simulation of Single Round Jet at Low Reynolds Number

Raj Narayan Gopalakrishnan<sup>1</sup>, Peter J. Disimile<sup>2</sup>

<sup>1</sup>Department of Aerospace Engineering, University of Cincinnati, Cincinnati, OH, USA 45221

<sup>2</sup>Department of Aerospace Engineering, University of Cincinnati, Cincinnati, OH, USA 45221

### ABSTRACT

Single axi-symmetric round jet flow was analyzed using computational techniques and validated with experimental results to establish the suitable turbulence model for simulation of low Reynolds number jets exiting from fully developed pipe. This work is performed as an initial study before computationally simulating multiple impinging jets. To this end a single round jet at Reynolds number of 7500 exiting from a fully developed pipe and entering into stationary air was modeled. Velocity and turbulence profiles were extracted from the simulation and validated with in-house experimental results. It was observed that although all the four turbulence models studied were able to closely predict the mean velocity field, they were not able to accurately predict the turbulence intensity distributions. From the models studied, it was concluded that SST k- $\omega$  model was the best turbulence model for simulating low Reynolds number jet flow exiting from fully developed pipe.

**Keywords:** CFD analysis, Low Reynolds number, Round Jets, Realizable k- $\epsilon$  model, SST k- $\omega$  model, Turbulence Intensity, Turbulence Model

### I. INTRODUCTION

Round jet flow is a form of free shear flow that has multitude of industrial applications, from water jet exiting the nozzles used by firemen for fire suppression to fuel jet in aircraft combustion chambers. Jet flow observed in nature, such as thermal plumes and volcanic exhausts also exhibit a circular profile and has been source of investigation for Bejan et al. [1]. The wide range of applications has ensured that a large number of research work was done to establish some of its underlying physics.

Round jet flows can exist in either a laminar or turbulent state; and for our current study we are studying turbulent axisymmetric round jets. An exhaustive review on turbulent round jets has been conducted by Ball et al. [2] in 2012, who examined the work of Tollmein (done in 1926) to round jet analysis done as recent as 2010. This work provided immense and valuable insight into the experimental and computational work done in the field of round jets. Their work briefly discusses the effect of initial conditions of the jet on similarity profile; which has been established by other authors. They also discuss the coherent structures observed in round jets and the length scales associated with the flow. At the end of their work, they have pointed out the parameters and physics of the round jet that still remain unknown; mainly the nature of interaction of the coherent structures and the mixing transition. It is indeed interesting to notice that even in 2012, the complete physics of such a ubiquitous fluid dynamic phenomenon is not completely understood.

Meanwhile, Kaushik et al. [3] and Dewan et al. [4] had performed a detailed survey on CFD (Computational Fluid Dynamics) treatment of round jet, which provided excellent insight into the recent computational works done in the field of research on round jets. While Kaushik et al. [3] discuss both laminar and turbulent jets, Dewan et al. [4] has concentrated on turbulent plane and round jets thereby providing a generalized view on jets and the recent research done.

One of the important aspect of round jets is the similarity nature of its mean velocity profile. It was believed from data obtained from experimental analysis that the round jet velocity profile exhibited self-similar nature, and that the profile was similar for all jets irrespective of the inlet flow conditions. It was George W. K. [5], who in his pivotal work established the dependence of turbulent scalar properties on inlet flow conditions using analytical methods. This work proved instrumental in initiating new generation of research where the initial conditions of jet flow and its impact were analyzed. Mi et al. [6] examined round jets with two different initial conditions (a top hat profile and a fully developed pipe flow) and were able to establish the dependence of turbulence scalar properties on initial conditions similar to that presented by George W. K. [5]. Similar study was conducted by Ferdman et al. [7] who studied the effect of initial conditions on velocity and turbulence characteristics. Their study displayed a dependence of decay rates of jets on initial flow condition. From these studies, it was concluded that the round jet velocity and turbulence profile has direct association with initial

conditions. Fellouah et al. [8] established that there was direct correlation between the mean velocity condition at inlet to the turbulence and Reynolds stress profiles downstream. Their observation was similar to those made by Dimotakis [9] who established a Reynolds number range of  $1-2 \times 10^4$  based on outer scale for the flow to become sustainably turbulent. These studies helped to establish the dependence of flow physics on the Reynolds number. From these studies, it was concluded that when validating computational results of axisymmetric round jet, unique data set data was acquired from specific experimental setup, where both initial conditions and Reynolds number matched. Any mismatch in boundary or flow conditions would affect data set quality and lead to a possible mismatch. Hence, work done by Landers [10] was used for validation since the experimental conditions including the initial flow profile generation and Reynolds number matched with the current study.

## II. COMPUTATIONAL METHODOLOGY

In the present work, the flow exiting a fully developed round pipe was used as the inlet condition for the single axis-symmetric round jet. Gopalakrishnan and Disimile [11] previously noted that the purpose for an autonomous pipe and jet simulation was to control the grid points in both the studies so that the simulations could be performed independently with a high level of mesh refinement and accuracy. The velocity profile obtained from the pipe flow simulation was validated with published results, whereby a considerable agreement was observed. This provided high confidence in the pipe flow solution, which was then used as the inlet boundary condition of the single jet simulation.

In the current study, a single round axis-symmetric jet was analyzed using Realizable k- $\epsilon$  model initially at Reynolds number = 7,500. Multiple meshes were generated to identify the smallest mesh setup by which the solution becomes independent of grid resolution. Once a grid independent solution was obtained, the result from the simulation was compared with in-house experimental results which indicated discrepancies in turbulence intensity data obtained between computational and experimental approach. This was further analyzed by performing the single jet analysis using other turbulence models and comparing the results.

## III. GEOMETRY AND MESH GENERATION

The reason for performing single jet CFD analysis was to gain a better understanding of the computational capabilities of current turbulence models in capturing the jet's free shear layer physics. Once adequate understanding was obtained with single jet, the most suitable turbulence model was selected to perform the analysis of two jets impinging at an angle. Work performed by Disimile et al. [12] on impinging jets has been taken as the validation source for impinging jet analysis, wherein a Reynolds number of 7500 was used. Hence for the single jet study, and the pipe flow study [11] which preceded this work; Reynolds number used was 7500. Disimile et al. [12] had used pipe internal diameter of 20 mm in their study, which was maintained in the present work and in Landers [10].

Since in the experimental conditions, the jet exiting the pipe mixes with a still ambient fluid (air); the geometry designed for the current study had to represent a similar setup. This was attained by keeping the boundaries very far from the jet path, so that the presence of any form of computational boundary would not manipulate the jet. With this consideration, the computational geometry was generated in form of frustum, with the pipe flow exit (and jet inlet) in the smaller section and the domain exit at the larger section. All the surfaces, including the curved periphery was modelled to allow flow of mass in either direction and was set as pressure outlet boundary conditions where reverse flow was permitted.

A pictorial representation of the geometry is shown in Figure 1. All surfaces other than inlet was modelled as pressure outlet. In order to maintain solution reliability, the domain was constructed with the smaller side of frustum with radius of 15D while the larger side had 25D as shown in Figure 1 and Figure 2.

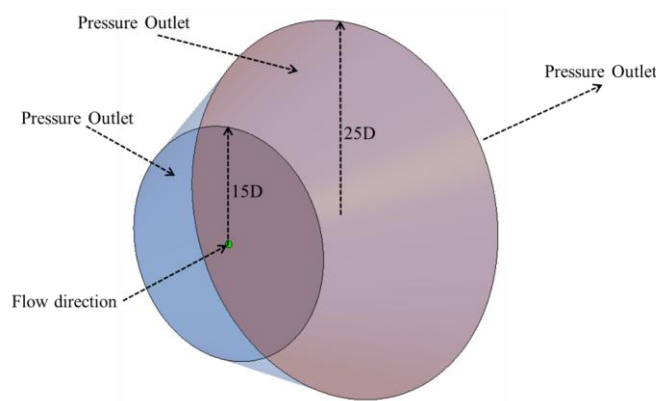


**Figure 1:** Geometry for single axis-symmetric jet simulation

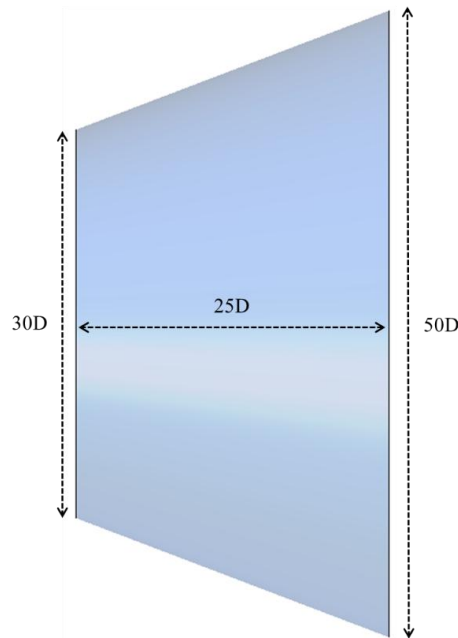


**Figure 2:** Side view of geometry for single axis-symmetric jet simulation

The axial flow length of  $25D$  was maintained for the flow to develop inside the geometry. Further downstream was not modelled or analyzed since the primary interest of this study was to simulate the near field physics of round jets. Once the geometry was designed and initial boundary conditions established, the next step involved in the analysis was grid generation. Two separate O-grids were used to capture the outer and inner periphery of the frustum as shown in Figure 3. It shows the mesh with node count of 4.3 million nodes.

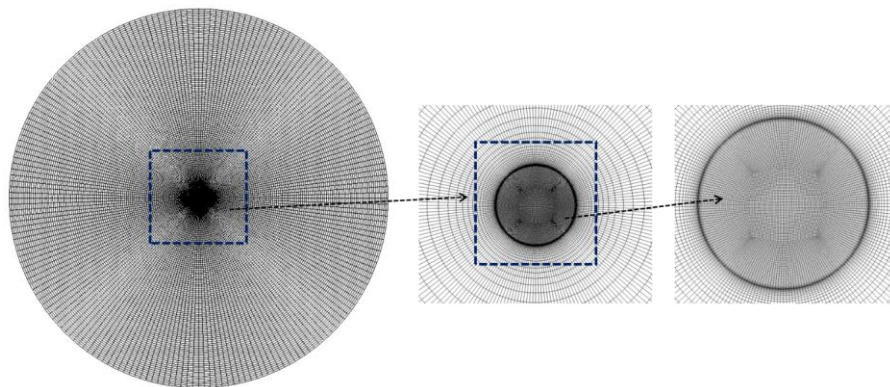


**Figure 3:** Front view and close-ups showing the mesh with 4.3 million nodes in detail

It can be observed in Figure 3 that the mesh close to the center (which is the pipe exit domain) is very fine when compared to the mesh at the periphery. This has been maintained for the accurate transfer of resulting flow data from the pipe simulation, since using a coarse mesh leads to data averaging.

The dark ring seen in the right most snapshot of the mesh indicates the boundary layer mesh within the pipe flow. In order to accurately capture of boundary layer physics, the first node height had to be reduced so that the distance from the wall in wall coordinates,  $y^+$  is closer to 1. This condition yielded a first node height of 0.036 mm in the pipe domain. Since the pipe domain exits into the jet domain, the same first node height was initially maintained into the jet domain. Figure 4 shows the side view of the mesh. As can be clearly observed, the central core region was captured with very fine mesh while mesh was allowed to grow coarser as it reached the periphery of the domain.

Various mesh quality checks using different parameters were performed to ensure that the mesh obtained was of adequate quality. Detailed description of the parameters and allowable limits for the same have been presented in [11]. For the current study, it was established that the aspect ratio never exceeded 100 (the maximum aspect ratio allowed by Ansys Fluent). Once a mesh with the required quality was generated, it was saved as \*.msh file from ICEM-CFD which was then input into the commercial finite volume solver, Ansys Fluent.

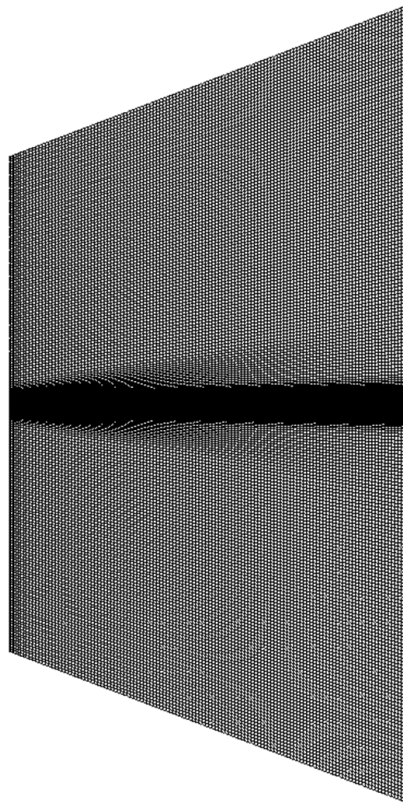


**Figure 4:** Side view of mesh for single axis-symmetric round jet

#### IV. CHOICE OF TURBULENCE MODELS

One of the primary concerns in this analysis was the ability of the turbulence models to reliably capture the physics of free shear flows. It was noted during literature review that certain models performed better for round jet flow when compared to others. Also, there were articles that implied the dependence of the flow field on initial conditions [7] and proposed that round jets cannot be accurately simulated easily with the turbulence models and parameters currently in use [13]. For the purpose of this study, four turbulence models were selected for examination; Realizable  $k$ - $\epsilon$  model, SST  $k$ - $\omega$  model, Standard  $k$ - $\epsilon$  model and Standard  $k$ - $\omega$  model. Studies comparing the efficacy of Realizable  $k$ - $\epsilon$  model with Standard  $k$ - $\epsilon$  model and Standard  $k$ - $\omega$  model were found and so was studies comparing SST  $k$ - $\omega$  model with Standard  $k$ - $\epsilon$  model and Standard  $k$ - $\omega$  model. But, no study comparing all these four models for turbulent round jets was found by the authors. Hence, this study provides insight into the area of choice of best turbulence model when simulating round jet flow exiting fully developed pipe at low Reynolds number. The turbulence models used in the current study is described in some details below.

##### 4.1 Realizable $k$ - $\epsilon$ model

Realizable  $k$ - $\epsilon$  model has been said to be modified to accurately predict the spread rate of planar and round jets. T.-H. Shih et al. [14] asserts that effect of rotation on both turbulent kinetic energy ( $k$ ) and eddy dissipation rate ( $\epsilon$ ) has been well captured in Realizable  $k$ - $\epsilon$  model. This is claimed to be a reason for the superior performance of Realizable  $k$ - $\epsilon$  model when compared with Standard  $k$ - $\epsilon$  model. The realizability condition implies: a) Turbulent shear stress satisfy Schwarz inequality and b) Non-negative values for normal stress. Also, Realizable  $k$ - $\epsilon$  model uses a variable for model coefficient  $C_\mu$  instead of using constant like Standard  $k$ - $\epsilon$  model.

##### 4.2 SST $k$ - $\omega$ model

SST  $k$ - $\omega$  model by Menter [15] has been found to perform better than Standard  $k$ - $\epsilon$  model for capturing round jet physics during literature review. The model, being a combination of Standard  $k$ - $\omega$  model in the boundary layer flow and Standard  $k$ - $\epsilon$  model for outer layer has been one of the most favorite go-to turbulence models in the CFD community. The near wall capability of Standard  $k$ - $\omega$  model combined with blending function which transforms it into Standard  $k$ - $\epsilon$  model in case of free shear flows makes it valid for wide range of applications, even in areas with adverse pressure gradients and separation regions.

#### 4.3 Standard k- $\epsilon$ model

Proposed in 1974 by Launder and Sharma [16], it is one of the most common and oldest turbulence model in use. It's a semi-empirical model with the turbulent kinetic energy (k) and dissipation rate ( $\epsilon$ ) based on model transport equations. It has been observed that the Standard k- $\epsilon$  model performs poorly in case of adverse pressure gradients. As further research provided conclusive evidence on the strength and weakness of the Standard k- $\epsilon$  model; modifications were made to it to improve its performance. Such modifications have led to the creation of few variations, of which two models are RNG k- $\epsilon$  model and Realizable k- $\epsilon$  model.

#### 4.4 Standard k- $\omega$ model

Standard k- $\omega$  model by Wilcox [17] is another popular model among CFD users. It is an empirical model based on model transport equations for the turbulence kinetic energy (k) and the specific dissipation rate ( $\omega$ ). The Standard k- $\omega$  model has better wall physics capturing capability than Standard k- $\epsilon$  model and can handle meshes with  $y^+$  closer to 1. Similar to Standard k- $\epsilon$  model, it has many weaknesses due to which modifications were made, which eventually lead to the creation of SST k- $\omega$  model.

### V. BOUNDARY CONDITIONS AND SOLVER SETUP

After choosing a turbulence model, the simulation requires the proper boundary conditions that will impart the real world environment to the simulation. The flow from fully developed pipe was to be used as the inlet boundary condition to the jet flow. Velocity and turbulence kinetic energy profiles as shown in Figure 5; were extracted from the outlet of pipe flow simulation and were provided as the input boundary condition. In order to simulate that the jet escaping into ambient fluid at atmospheric conditions, the outlet condition for the round jet simulation was set as pressure outlet at ambient pressure. The periphery of the domain was also set as pressure outlet condition at ambient pressure in order to replicate natural conditions. This allowed for entrainment of the ambient fluid from all the directions. Air at ambient temperature and pressure was used as the working fluid. Solver settings used by authors can be found in previous pipe study [11]. SIMPLE algorithm was utilized for pressure-velocity coupling with the 2nd order Upwind scheme used for spatial discretization. A convergence criteria of  $1e-6$  was used to confirm that the solution had fully converged with minimal possible error. Once the residuals for the convergence criteria were satisfied, the run was stopped and the results file extracted to be post processed.

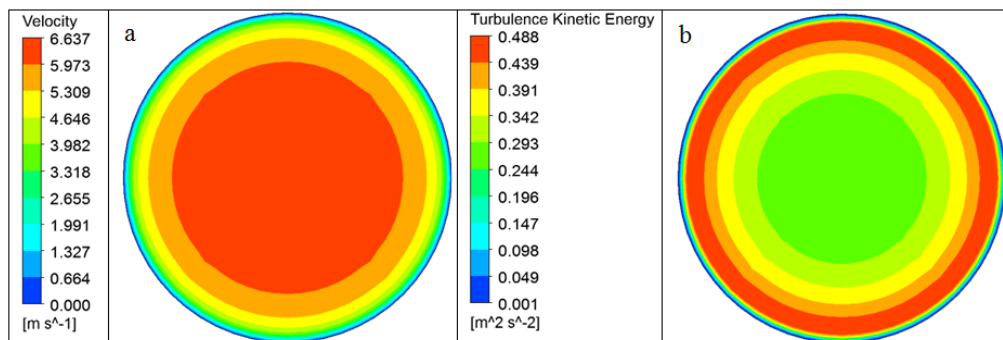


**Figure 5:** a) Velocity and b) Turbulence Kinetic energy used as inlet condition for the round jet

### VI. GRID INDEPENDENCE

As shown in the earlier pipe study performed by the authors, Gopalakrishnan and Disimile [11]; it is imperative that the solutions obtained from any CFD analysis be resolved over multiple meshes in order to ascertain that the solution achieved is not dependent on the grid size used. Assessing grid independence is carried out by running simulations using multiple mesh configurations for the same geometry and boundary conditions and observing the change in target parameters as the mesh is altered. Ideally, a very small mesh is generated initially which satisfies the bare minimum mesh quality requirements (as discussed in [11]). Based on this mesh, further meshes are typically generated by refining the mesh size over every iteration. The results from all these meshes are compared, and the mesh size beyond which no significant change in target parameter occurs for any variation in mesh size is considered as the point of grid independence. This mesh at the point of grid independence is then taken as the minimal mesh required to obtain a node independent solution for that particular geometry and simulation setup.

For the current study, six (6) different mesh geometries were generated starting from 0.25 million nodes. All the analysis for the grid independence study was performed using Realizable k- $\epsilon$  turbulence model. The mesh at the inlet of the jet domain was matched with the mesh from the outlet of the pipe used in [11] and the initial mesh height of 0.036 mm into the jet domain was initially maintained. This was required for a smooth continuation of

mesh from the pipe outlet and for the accurate transfer of flow variables without any interpolation or averaging. However, starting with a very low mesh node count and maintaining such small grid spacing at center yielded regions with coarse mesh and high aspect ratio. In the current study those regions were successfully maintained at the periphery of the domain, ie away from the area of interest.

This can be clearly observed in Figure 6 where the mesh close to the center of the domain is maintained at a height of 0.036mm whereas the peripheral mesh was on the order of millimeters. This meshing philosophy was applied in order to keep the starting node count low. As meshing iterations proceeded with the generation of finer meshes, the mesh along the periphery was refined while adding nodes in the central region as shown in Figure 6.

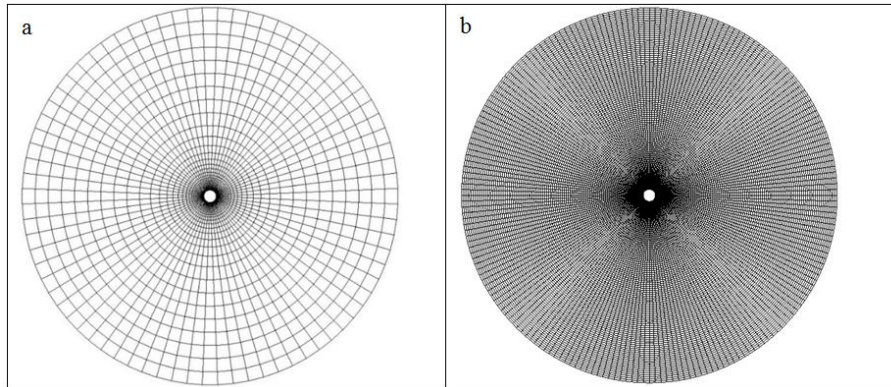


**Figure 6:**Front view of grid with a) 0.25 million nodes and b) 4.3 million nodes

A similar mesh refinement tactic was applied along the axial flow direction thereby reducing the aspect ratio with every iteration of mesh enhancement. Impact of this refinement strategy can be clearly observed in Figure 7.

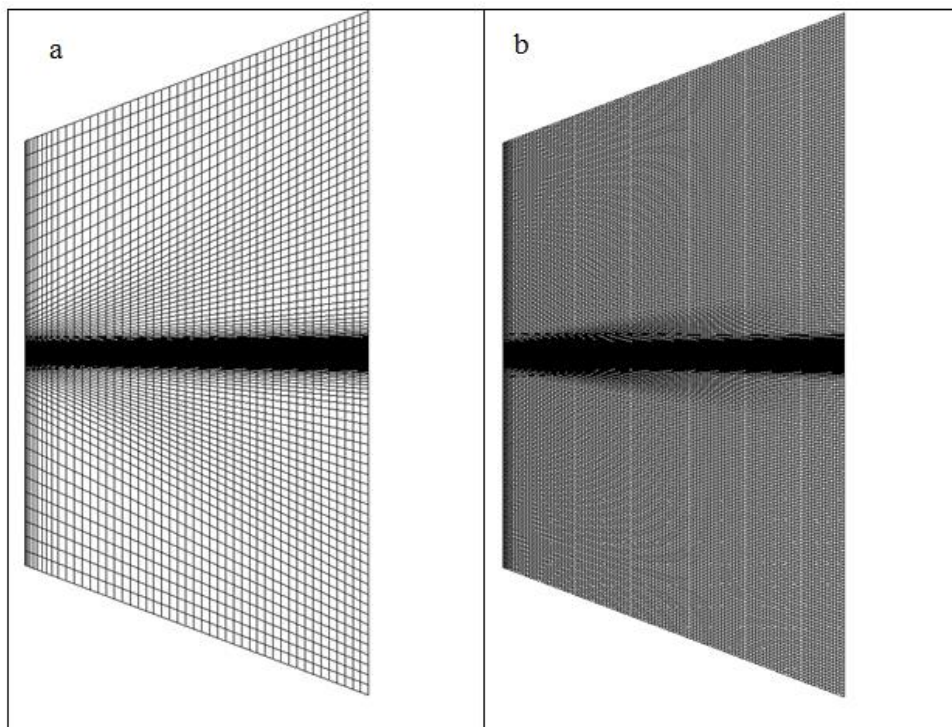


**Figure 7 :** Side view of central plane for grid a) 0.25 million nodes and b) 4.3 million nodes

Once all the test cases were successfully converged, the results from the analyses were extracted for post processing. Mean velocity and turbulence kinetic energy (TKE) were obtained from all the mesh configurations and plotted systematically to identify the point of grid independence as shown in Figure 8 and Figure 9.

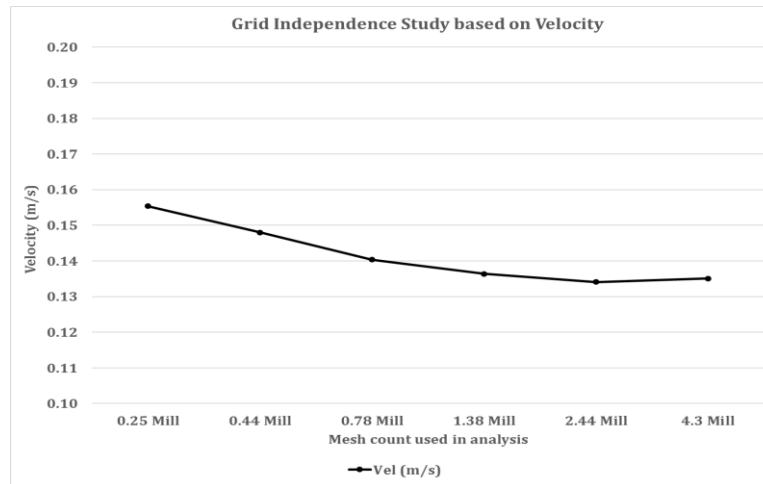


Figure 8: Grid Independence based on Mean Velocity value

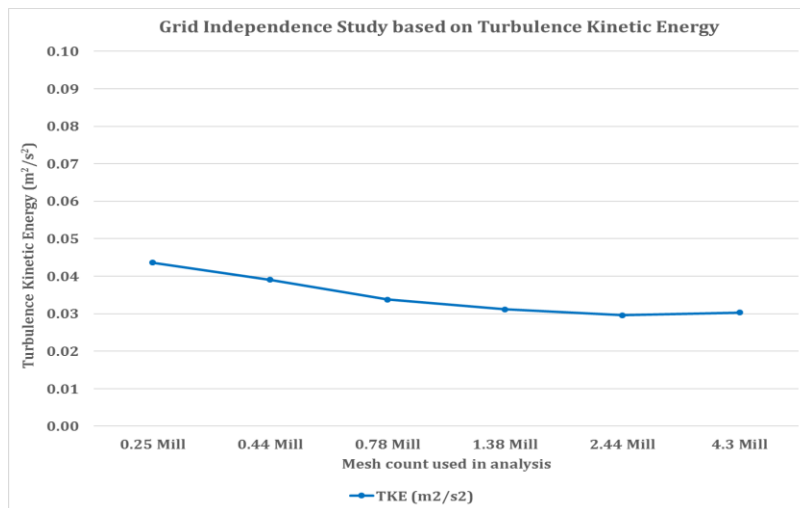


Figure 9: Grid Independence based on Turbulence Kinetic energy value

It is evident from Figure 8 and Figure 9 that the solution becomes independent of the grid size at around 1.38 million nodes since no significant change was observed in the velocity or turbulence kinetic energy value beyond 1.38 million nodes, even with tripling the mesh size. The maximum variation from 1.38 million nodes is of the order of 1.7% in terms of mean velocity and 5% in terms of turbulence kinetic energy for mesh size above 1.38 million nodes as seen in Table 1. These values are negligible when compared to the variation observed in experimental data [10] which indicated a range of 10-18% fluctuation in the calculation of mean velocity values and 22-41% fluctuation in the calculation of turbulence kinetic energy values for different experimental setup in the case of single jet analysis.

Table 1 : Grid Independence data

Grid Independence Study			Difference from 1.38 million node case		% Difference from 1.38 million node case	
	Vel (m/s)	TKE (m2/s2)	Vel (m/s)	TKE (m2/s2)	Vel (m/s)	TKE (m2/s2)
0.25 Mill	0.1554	0.0436	0.0189	0.0125	13.8836	39.9865
0.44 Mill	0.1480	0.0391	0.0116	0.0079	8.4796	25.3214
0.78 Mill	0.1404	0.0338	0.0040	0.0026	2.9040	8.3026
1.38 Mill	0.1364	0.0312	0.0000	0.0000	0.0000	0.0000
2.44 Mill	0.1341	0.0296	-0.0023	-0.0016	-1.7191	-5.0892
4.3 Mill	0.1351	0.0303	-0.0013	-0.0009	-0.9762	-2.8290

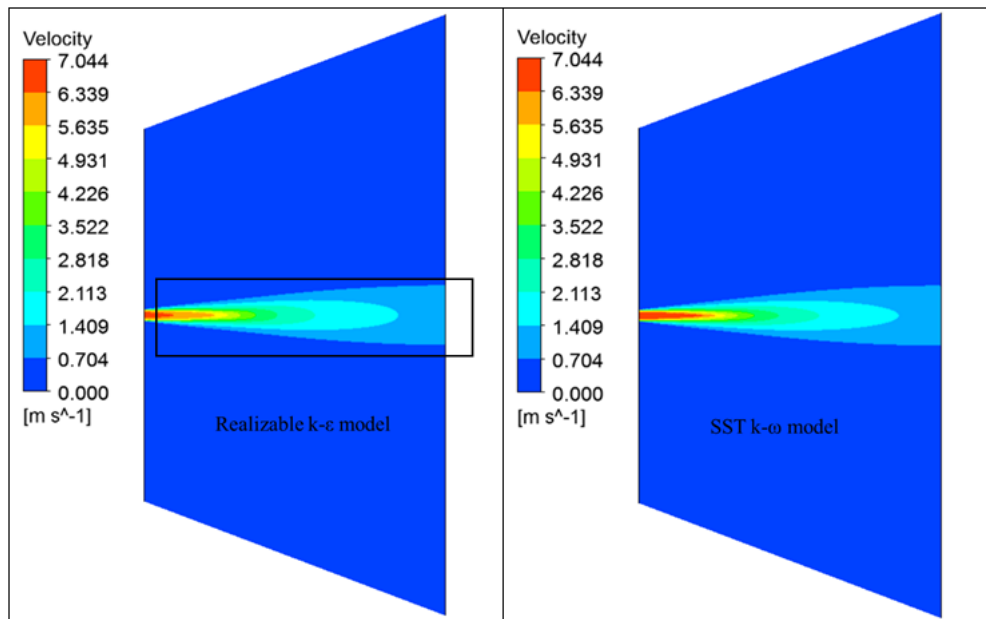
Hence for further analyses, 1.38 million node mesh was considered as the baseline mesh. Using this mesh, a single axisymmetric turbulent jet was simulated as exiting a long constant diameter round pipe with fully developed turbulent velocity profile.

### 7. Effect of Turbulence Models

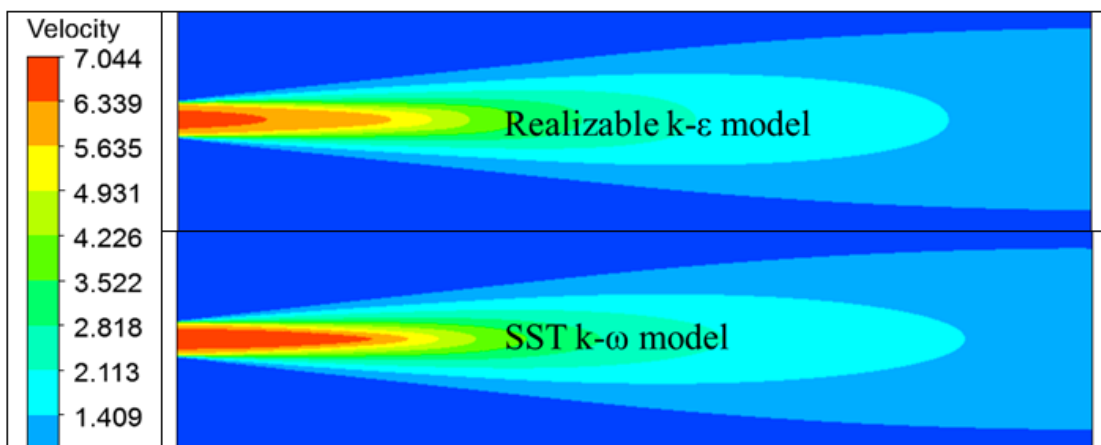
The single jet analysis was initially performed using Realizable  $k-\epsilon$  model and was further simulated using SST  $k-\omega$  model, Standard  $k-\epsilon$  model and Standard  $k-\omega$  model. It has to be noted that the choice of Realizable  $k-\epsilon$  model as the first model used for analysis was based on the literature review, which claimed that the performance of Realizable  $k-\epsilon$  model was adapted specifically for accurate prediction of the spread rate of round jets. During literature review, it was also noted that the SST  $k-\omega$  model's performance was claimed superior to that of Standard  $k-\epsilon$  model and Standard  $k-\omega$  model [Menter [15]]. But a research work comparing the performance of SST  $k-\omega$  model and Realizable  $k-\epsilon$  model for single round jets was not found during literature survey.

### 8. Comparison of the velocity profiles from different turbulence models against in-house experimental results

From Figure 10, it can be observed that there exists significant difference in the distribution of area of high velocity (as shown within the demarcated region) when calculated by four turbulence models. It was imperative to look closely into this zone to establish the accuracy of each turbulence model. Figure 11 gives the zoomed in look at demarcated zone. A general trend observed was that the epsilon based turbulence models generated smaller regions of higher velocity when compared to omega based models. Of the four turbulence models under study; Standard  $k-\omega$  model seems to have the largest zone with maximum velocity, denoting lower turbulence dissipation.



**Figure 10:** Velocity contour along central plane for single axis-symmetric jet obtained using various turbulence models



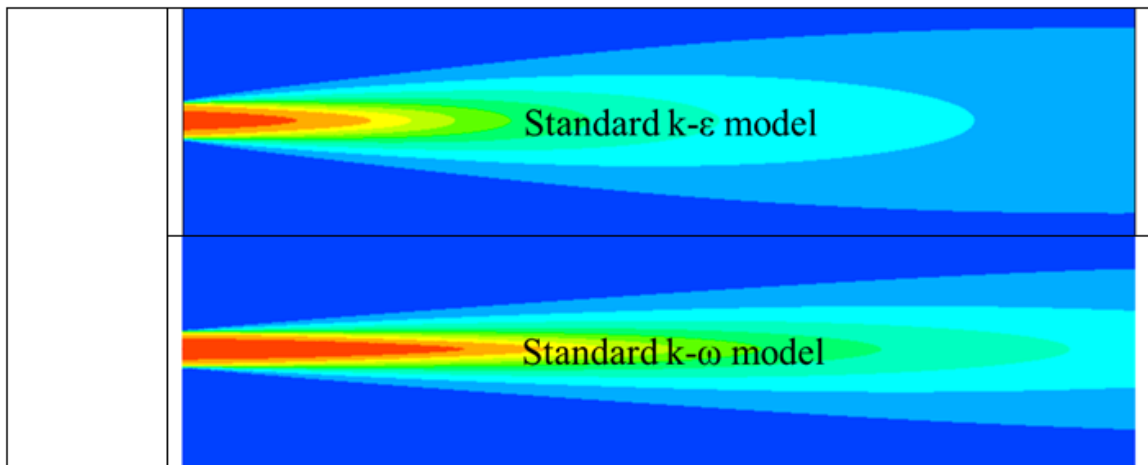


**Figure 11:** Zoomed view of velocity contour along central plane for single axis-symmetric jet obtained using various turbulence models

In order to obtain a holistic understanding of the general trend of velocity at central zone, velocity profiles were extracted from central line and different locations downstream of pipe exit. These profiles were compared with data from Landers [10] in order to establish the turbulence model which provided solution closest to the experimental result.

Velocity data extracted from axial central line was normalized with maximum velocity along the center line (which occurs at the exit of the pipe flow) and was plotted over axial distance measured in pipe diameters. From Figure 12; we notice that the Standard  $k-\omega$  model follows a more deviated path when compared to the three other remaining models. This consistent deviation of results obtained for Standard  $k-\omega$  model demands further investigation on the performance of the model. Another key-point to be noted from the Figure 12 is that the performance of SST  $k-\omega$  model, Realizable  $k-\epsilon$  model and Standard  $k-\epsilon$  model are very similar except in the region between 5D to 10D from the pipe exit. This may be due to the breakdown of potential core in that region suggesting different models simulates this region differently.

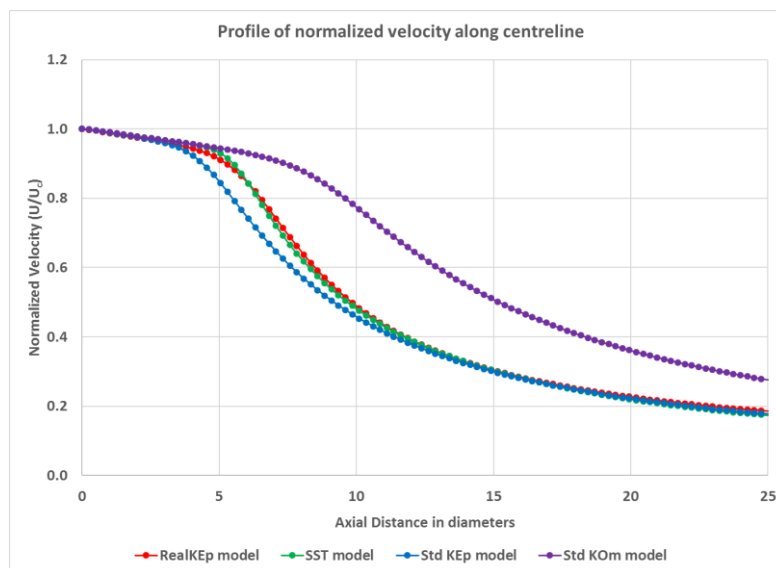


**Figure 12 :** Profile of normalized velocity along centerline

Initially, velocity data extracted from different location downstream of the pipe exit were plotted against data from Landers [10] as shown in Figure 13 to Figure 16. The general trend observed was that the performance of Realizable  $k-\epsilon$  model and SST  $k-\omega$  model closely matched each other with Standard  $k-\epsilon$  model being another close contender. It has to be noted that, beyond 6D; data from experimental study also showed a wider spread. Meanwhile, the Standard  $k-\omega$  model showed the maximum deviation from the experimental data at 9D and 10.33D. As seen in Figure 15 and Figure 16, the Standard  $k-\omega$  model starts to deviate from the general trend while the 3 other turbulence models illustrate similar results.

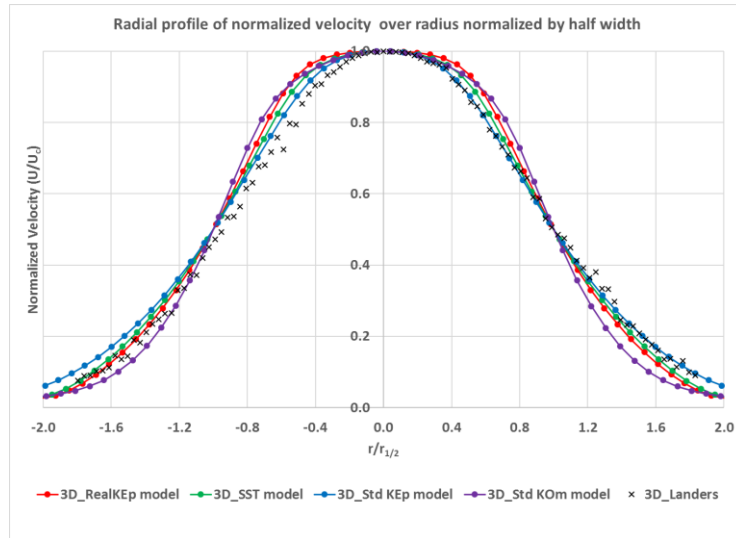


**Figure 13:** Radial profile of normalized velocity over radius normalized by half width at 3D from pipe exit

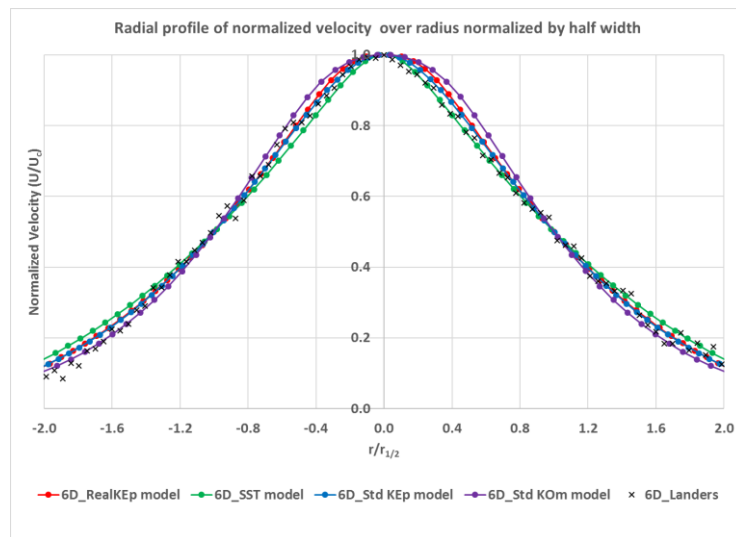


**Figure 14:** Radial profile of normalized velocity over radius normalized by half width at 6D from pipe exit

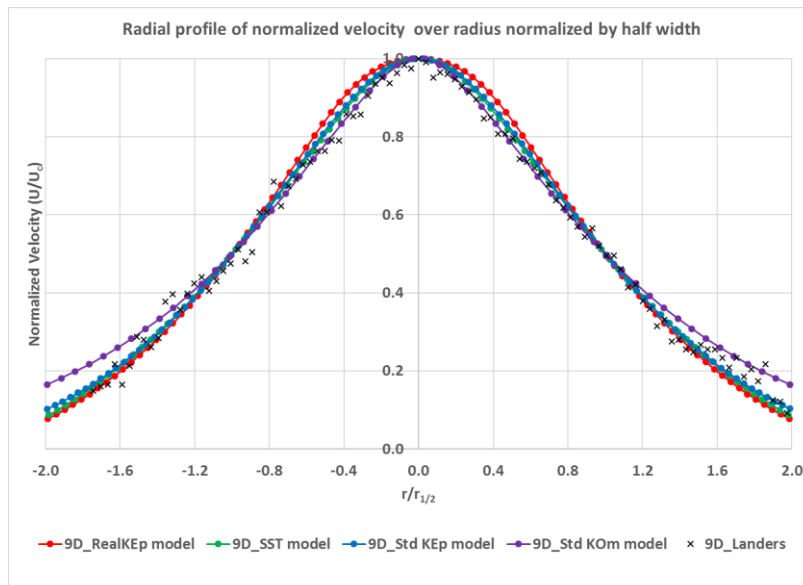


**Figure 15:** Radial profile of normalized velocity over radius normalized by half width at 9D from pipe exit

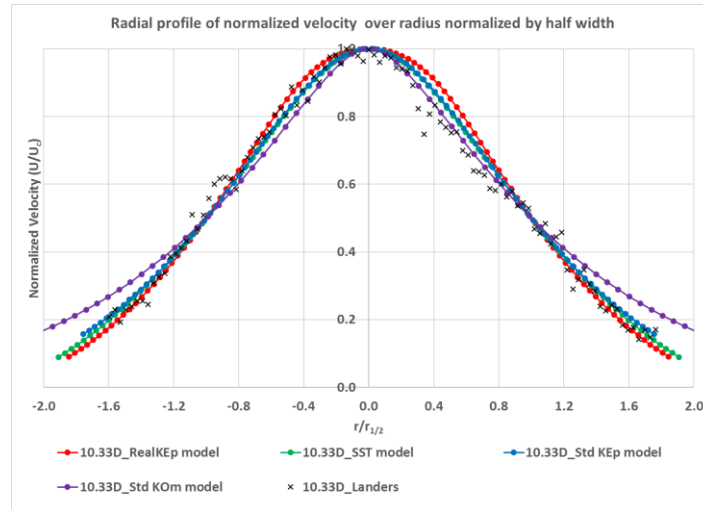
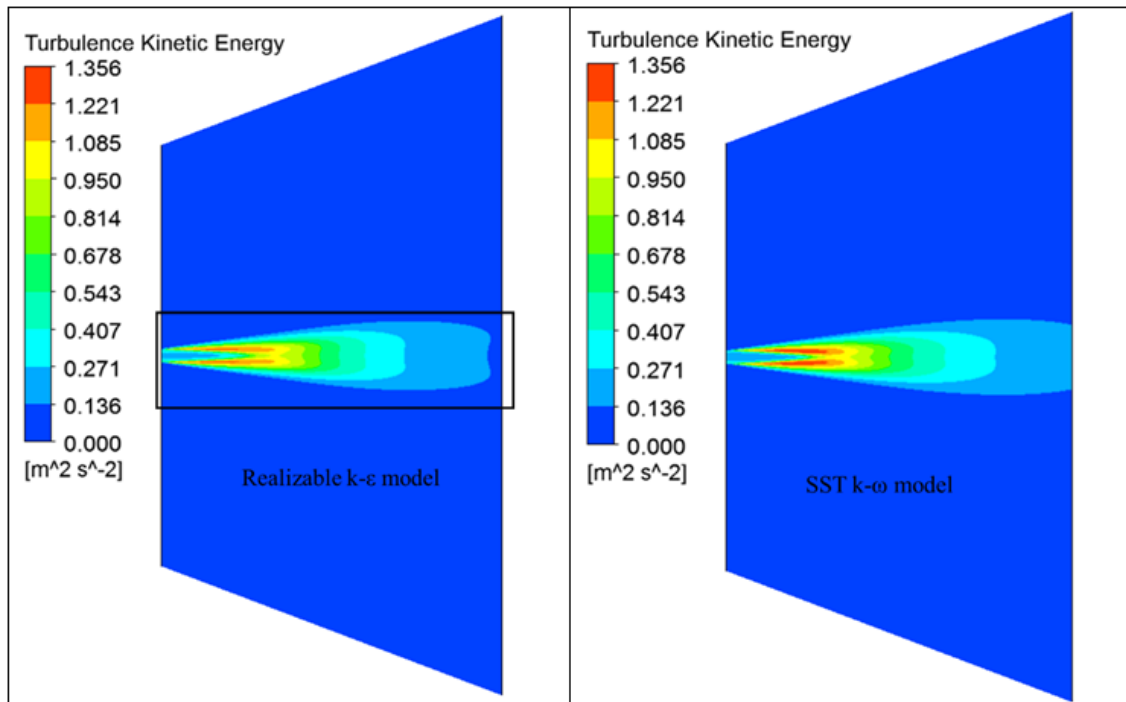


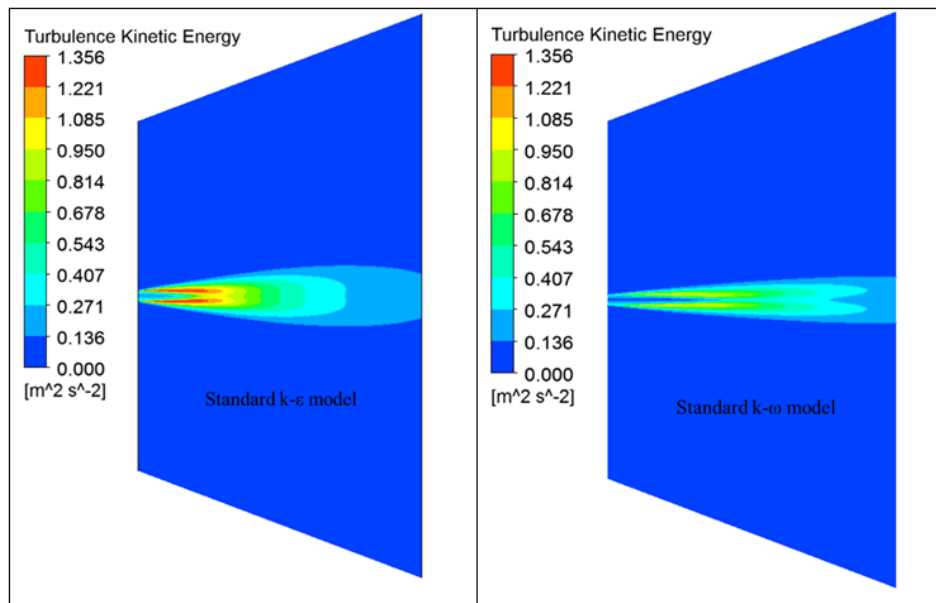
**Figure 16:** Radial profile of normalized velocity over radius normalized by half width at 10.33D from pipe exit

## VII. COMPARISON OF TURBULENCE PROFILE FROM DIFFERENT TURBULENCE MODELS WITH IN-HOUSE EXPERIMENTAL RESULTS

It was concluded that the performance of the four turbulence models was comparable in accuracy when considering the mean velocity. However, different parameters need to be examined, in order to distinguish the most suitable model for the current single simulation and future impinging jet study. Turbulence intensity was identified as a suitable parameter in previously established works and hence it was taken for consideration in the present study also.

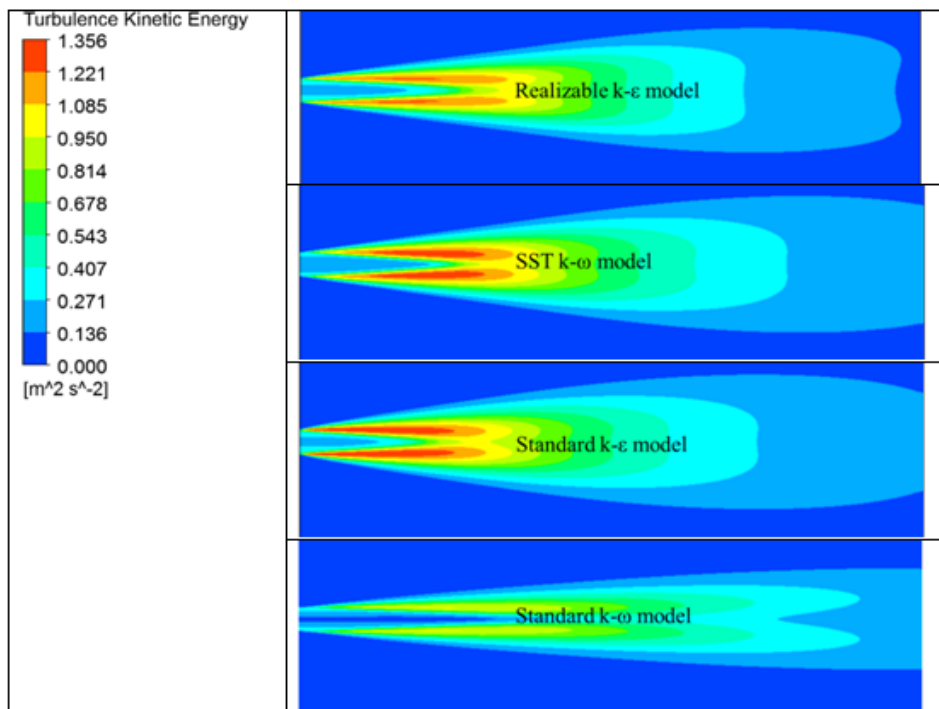
As done previously, central plane was considered for extraction of data for plotting contours and profiles. Turbulence intensity data was extracted along the center line and at various locations downstream of pipe exit and compared with experimental data obtained from [10]. The turbulence kinetic energy (TKE) contours along the central plane is shown in Figure 17. It is observed that there exists significant difference in the simulation of turbulence by the four turbulence models. While the SST k- $\omega$  model and the Standard k- $\epsilon$  model displayed similar performance for TKE parameter, Realizable k- $\epsilon$  model and Standard k- $\omega$  model predicted lower values of TKE, with Standard k- $\omega$  model predicting the lowest.





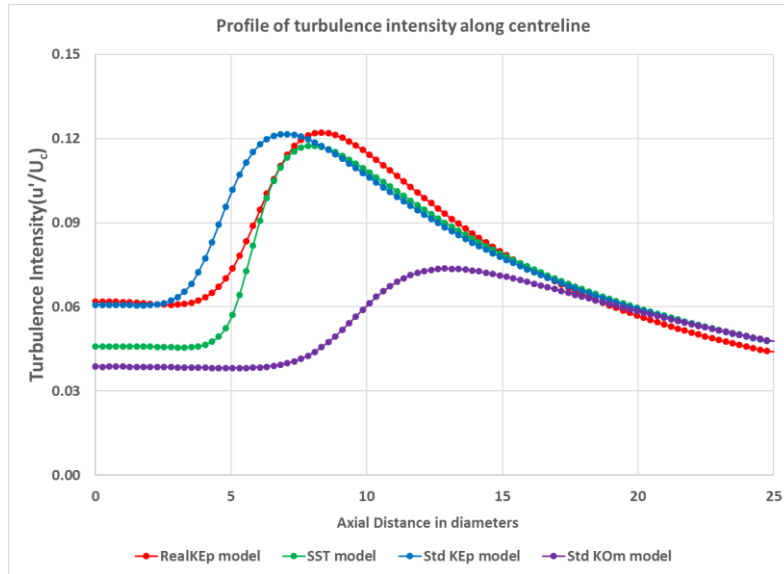
**Figure 17:** Turbulence kinetic energy contour along central plane for single axis-symmetric jet obtained using various turbulence models

Figure 18 gives the zoomed in look at demarcated zone shown in Figure 17, so that a better judgement of the profile can be obtained. The presence of low turbulence region in the middle of the jet for Standard  $k-\omega$  model indicates that the model predicts lower turbulence in the high velocity region.



**Figure 18:** Zoomed view of turbulence kinetic energy contour along central plane for single axis-symmetric jet obtained using various turbulence models

For obtaining clear understanding of the nature of turbulence simulated by the different models, it was imperative to look at the turbulence intensity (TI) data at different locations and compare it with experimental results from [10]. Initially, TI for different models were plotted along the center line and compared as shown in Figure 19. Again, the Standard  $k-\omega$  model stands as the odd-one-out, predicting very low values of TI until 18D downstream of pipe exit.



**Figure 19 :** Profile of turbulence intensity along center line

An interesting observation can be made regarding Realizable  $k-\epsilon$  model was that beyond 18D, the TI dips the most for that model. This can be observed in Figure 18 also, as the contour for Realizable  $k-\epsilon$  model alone indicates the presence of lower TKE zone near the right end of the zone. This needed to be further analyzed to ensure that confidence can be assigned to that model.

Warda et al. [18] had used relative turbulence intensity (RTI) instead of normal turbulence intensity in their study. This motivated the calculation of RTI profile for various turbulence models. It can be observed in Figure 20 that the RTI values obtained for all 3 models except Realizable  $k-\epsilon$  model showed similar trend of initially peaking to a maximum value and then become constant (similar to the trend shown by Warda et al. [18]) while Realizable  $k-\epsilon$  model predicted an initial cresting and then slowly decreasing. The trend of reduction in RTI after reaching a maximum value seems to indicate underlying inaccuracy in capturing the turbulence physics by the Realizable  $k-\epsilon$  model.

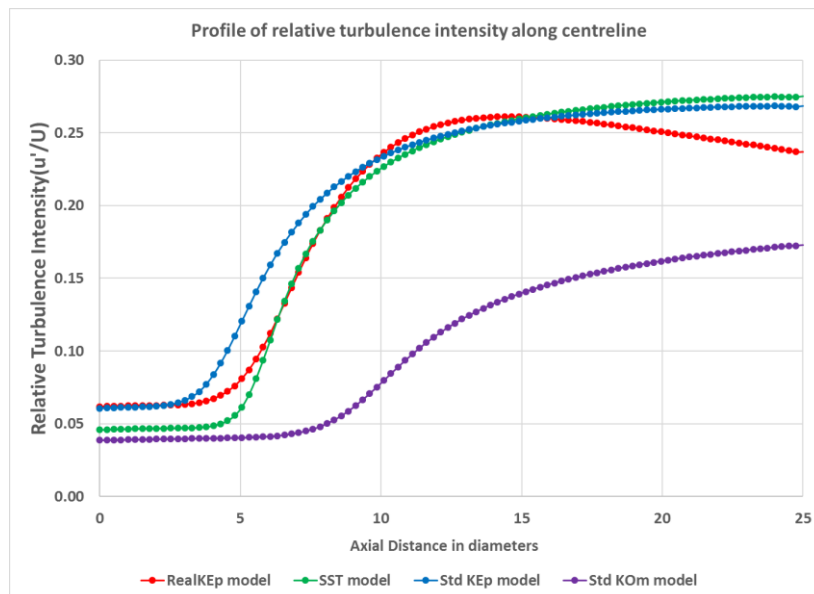


**Figure 20:** Profile of relative turbulence intensity along center line

The need to further ascertain the performance of Realizable  $k-\epsilon$  model in predicting TI parameter was recognized and TI data profiles were extracted at locations 3D, 6D, 9D and 10.33D from pipe exit for comparison and validation. Again, the performance of Realizable  $k-\epsilon$  model and SST  $k-\omega$  model were close to one another, with Standard  $k-\epsilon$  model being the next close model. Standard  $k-\omega$  model, as observed in other scenarios, performed differently.

Figure 21 to Figure 24 shows the radial profile of TI at different locations downstream of pipe exit. It is noted that the Realizable k- $\epsilon$  model and SST k- $\omega$  model were able to predict the TI value at 3D and 6D with some success. Standard k- $\epsilon$  model was able to closely predict the TI value only at 3D, while Standard k- $\omega$  model performed poorly in all locations. Beyond 6D, no model was able to accurately predict the TI for single round jet even though they were able to predict the general trend (except Standard k- $\omega$  model). All models except Standard k- $\omega$  model either correctly or over-predicts TI while Standard k- $\omega$  model under-predicts it at all the locations.

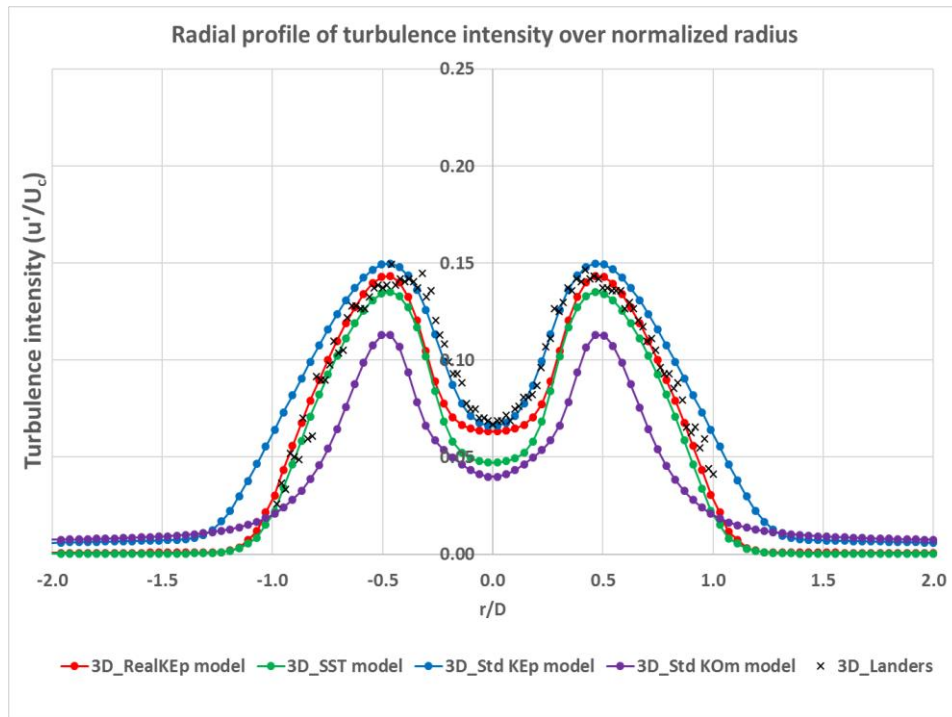


**Figure 21:** Radial profile of turbulence intensity at 3D from pipe exit

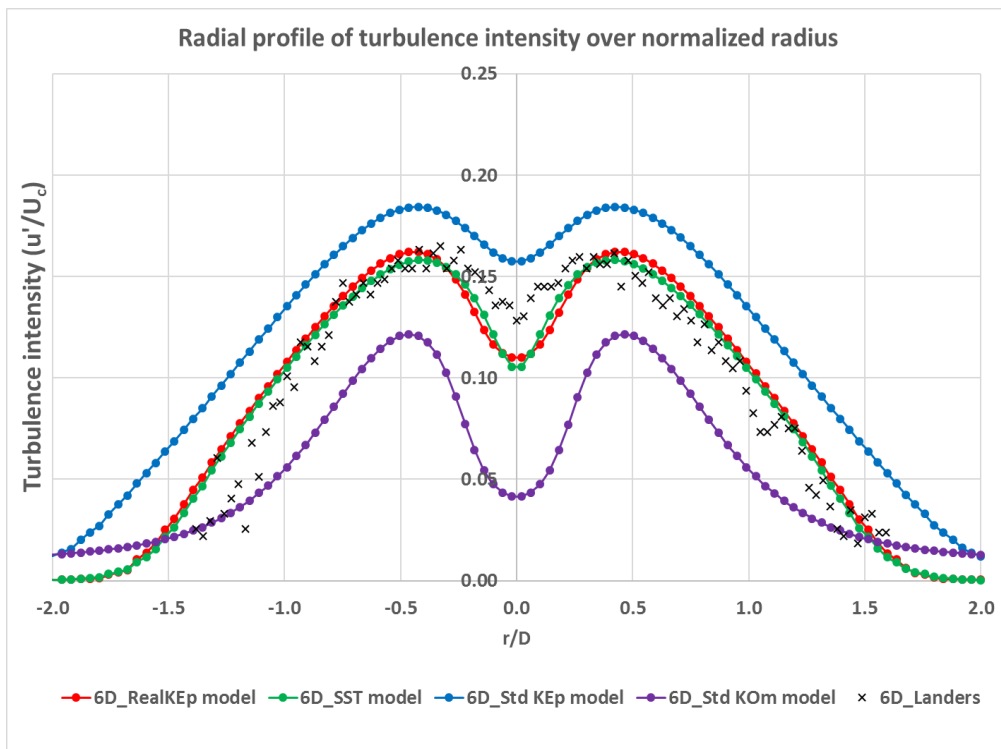


**Figure 22:** Radial profile of turbulence intensity at 6D from pipe exit

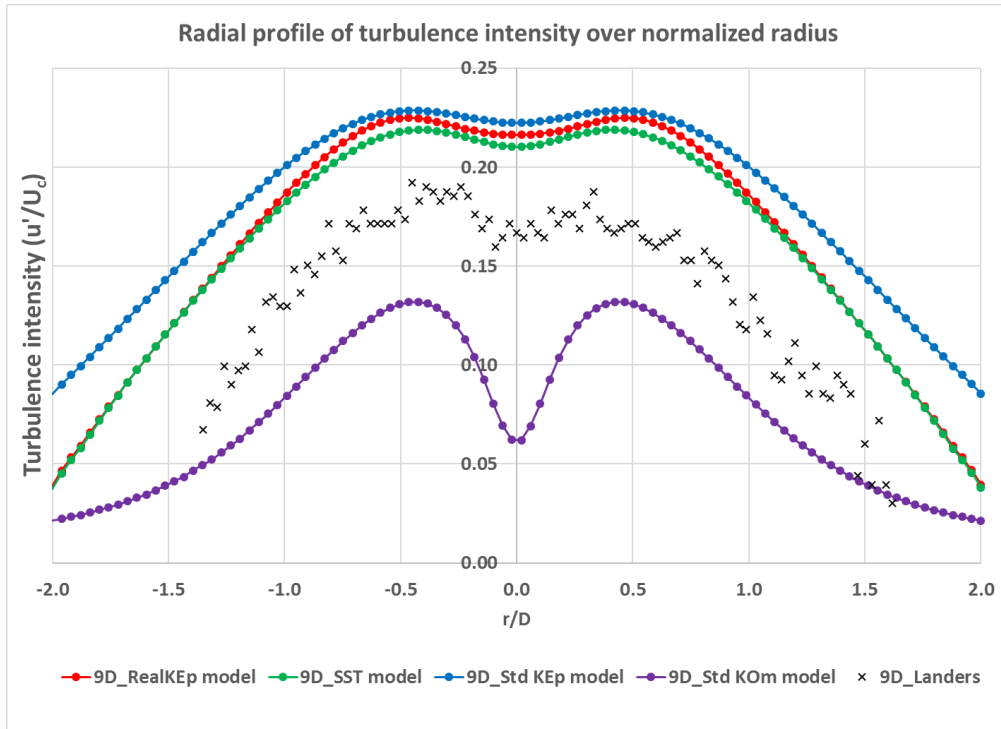


**Figure 23:** Radial profile of turbulence intensity at 9D from pipe exit

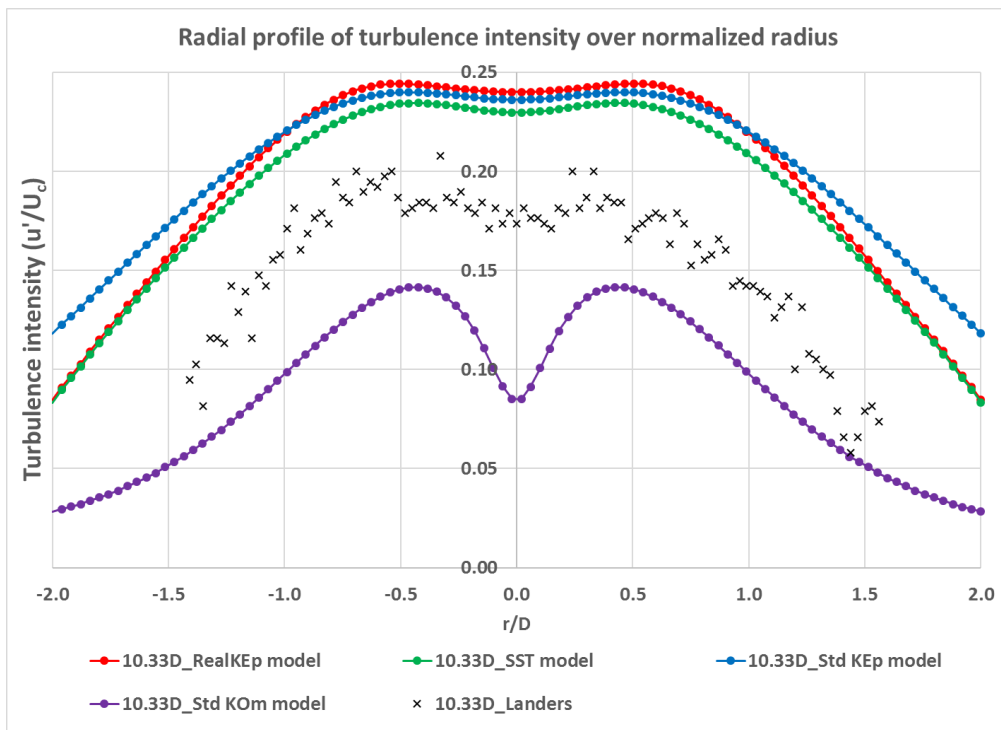


**Figure 24:** Radial profile of turbulence intensity at 10.33D from pipe exit

From the current results, it was concluded that the performance of Standard  $k-\omega$  model was not adequate enough to properly model the physics of single axis-symmetric round jet. Hence, it was decided to forego the Standard  $k-\omega$  model from future consideration. Since the performance of Realizable  $k-\epsilon$  model and SST  $k-\omega$  model were comparable (except for the inaccuracy of Realizable  $k-\epsilon$  model in calculating relative turbulence intensity near the end of the domain), it was deemed that SST  $k-\omega$  model was the better of the two. Also, performance of Standard  $k-\epsilon$  model and SST  $k-\omega$  model were quite comparable (except for Standard  $k-\epsilon$  model over-predicting turbulence intensity at 6D from pipe exit). From these observations, it was determined to use SST model alone to analyze impinging round jets.

## VIII. SUMMARY

Single jet simulations and analyses were performed at a Reynolds number of 7500 using various turbulence models to evaluate the performance of each model. This was done in order to determine the best possible turbulence model for a low Reynolds number round jet exiting from fully developed pipe flow. Based on the results from this study, jets impinging at an angle will be modeled in the next phase of analysis using the turbulence model that was found superior. Initially, grid independence was performed using Realizable  $k-\epsilon$  model to ensure that the solution obtained was independent of the grid size used. This was attained by performing the simulation using a very small mesh (0.25 million nodes) and gradually increasing the node count. It was found that beyond 1.38 million nodes, the solution did not show much dependence on the grid count, with only 2% difference in velocity and 5% difference in turbulence kinetic energy (TKE) with almost threefold increase in node count. Hence, for the purpose of single axis-symmetric round jets; 1.38 million node mesh was taken as the grid independent mesh for the current Reynolds number and simulation setup.

It was observed that all the turbulence models performed well in case of mean velocity profile (with Standard  $k-\omega$  model showing slight fluctuation at 10.33D). But, while plotting TI; it was observed that none of the turbulence models were able to accurately predict the TI values beyond 6D. Standard  $k-\omega$  model was found to under predict TI values at all the locations, while Realizable  $k-\epsilon$  model and SST  $k-\omega$  model were able to predict TI values till 6D. The performance of Standard  $k-\epsilon$  model was comparable with that of Realizable  $k-\epsilon$  model and SST  $k-\omega$  model. It was concluded that for the simulation of round axis-symmetric jets originating from a fully developed pipe flow at low Reynolds numbers, the SST  $k-\omega$  model was the best model to be used and Standard  $k-\omega$  model may be the least appropriate model.

### Nomenclature

$U_c$  – Centreline Velocity (m/s)

$U$  – Local Velocity (m/s)

$D$  – Diameter

$k$  – Turbulence kinetic energy ( $m^2/s^2$ )

$\epsilon$  – Dissipation rate ( $m^2/s^3$ )

$\omega$  – Specific Dissipation Rate ( $s^{-1}$ )

$r/2$  – Jet half width (m)

## REFERENCES

- [1]. Bejan, A., Ziaei, S. and Lorente, S., "Evolution: Why all plumes and jets evolve to round cross sections," Scientific Reports, vol. 04, no. 23, 2014.
- [2]. C. Ball, H. Fellouah and A. Pollard, "The flow field in turbulent round free jets," Progress in Aerospace Sciences, vol. 50, pp. 1-26, 2012.
- [3]. M. Kaushik, R. Kumar and G. Humrutha, "Review of Computational Fluid Dynamics Studies on Jets," American Journal of Fluid Dynamics, pp. 1-11, 2015.
- [4]. A. Dewan, M. Pathak and A. K. Dass, "A survey of selected literature on important flow properties and computational fluid dynamics treatments of incompressible turbulent plane and round jets in quiescent ambient," Indian Journal of Engineering and Materials Sciences (IJEMS), vol. 13, pp. 180-194, 2006.
- [5]. W. K. George, "The self-preservation of turbulent flows and its relation to initial conditions and coherent structures," Advances in turbulence, pp. 39-73, 1989.
- [6]. MI, J., NOBES, D.S. and NATHAN, G.J., "Influence of jet exit conditions on the passive scalar field of an axisymmetric free jet," Journal of Fluid Mechanics, vol. 432, pp. 91-125, 2001.
- [7]. E. Ferdman, M. V. Otugen and S. Kim, "Effect of Initial Velocity Profile on the Development of Round Jets," Journal of Propulsion and Power, vol. 16, no. 4, pp. 676-686, 2000.
- [8]. H. Fellouah, C. Ball and A. Pollard, "Reynolds number effects within the development region of a turbulent round free jet," International Journal of Heat and Mass Transfer, vol. 52, no. 17-18, pp. 3943-3954, 2009.
- [9]. P. E. Dimotakis, "The mixing transition in turbulent flows," Journal of Fluid Mechanics, vol. 409, pp. 69-98, 2000.
- [10]. B. Landers, "Mixing Characteristics of Turbulent Twin Impinging Axisymmetric Jets at Various Impingement Angles," Electronic Thesis or Dissertation, p. <https://etd.ohiolink.edu/>, 2016.
- [11]. R. N. Gopalakrishnan and P. Disimile, "Development of Inlet Boundary Condition for Accurate Multi-Jet Simulations," International Journal of Mechanical Engineering (IJME), 2016.
- [12]. P. J. Disimile, E. Savory and N. Toy, "Mixing characteristics of twin impinging circular jets," Journal of Propulsion and Power, 1995.
- [13]. S. B. Pope, "An explanation of the turbulent round-jet/plane-jet anomaly," AIAA Journal, vol. 16, no. 3, pp. 279-281, 1978.
- [14]. T.-H. Shih, W.W. Liou, A. Shabbir, Z. Yang and J. Zhu, "A New  $k-\epsilon$  Eddy Viscosity Model for High Reynolds Number Turbulent Flows-Model Development and Validation," NASA Technical Memorandum, Vols. ICOMP 94-21, 1994.
- [15]. F. R. Menter, "Two-Equation Eddy-Viscosity Turbulence Models for Engineering Applications," AIAA Journal, vol. 32, no. 8, pp. 1598-1605, 1994.
- [16]. B. E. Launder and B. I. Sharma, "Application of the Energy Dissipation Model of Turbulence to the Calculation of Flow Near a Spinning Disc," Letters in Heat and Mass Transfer, vol. 1, no. 2, pp. 131-138, 1974.
- [17]. D. Wilcox, "Re-assessment of the scale-determining equation for advanced turbulence models," AIAA Journal, vol. 26, no. 11, pp. 1299-1310, 1988.
- [18]. H. Warda, S. Kassab, K. Elshorbagy and E. Elsaadawy, "An experimental investigation of the near-field region of free turbulent round central and annular jets," Flow Measurement and Instrumentation, vol. 10, no. 1, pp. 1-14, 1999.
- [19]. D. Yoder, J. DeBonis and N. Georgiadis, "Modeling of turbulent free shear flows," Computers & Fluids, vol. 117, pp. 212-232, 2015.